

FAA-RD-72-77

**Project Report
ATC-13**

Parallel Approach Surveillance

**J. B. Allen
E. J. Denlinger**

14 August 1972

Lincoln Laboratory
MASSACHUSETTS INSTITUTE OF TECHNOLOGY
LEXINGTON, MASSACHUSETTS



Prepared for the Federal Aviation Administration,
Washington, D.C. 20591

This document is available to the public through
the National Technical Information Service,
Springfield, VA 22161

This document is disseminated under the sponsorship of the Department of Transportation in the interest of information exchange. The United States Government assumes no liability for its contents or use thereof.

1. Report No. FAA-RD-72-77	2. Government Accession No.	3. Recipient's Catalog No.	
4. Title and Subtitle Parallel Approach Surveillance		5. Report Date 14 August 1972	6. Performing Organization Code
7. Author(s) J.B. Allen, E.J. Denlinger		8. Performing Organization Report No. ATC-13	
9. Performing Organization Name and Address Massachusetts Institute of Technology Lincoln Laboratory P.O. Box 73 Lexington, Massachusetts 02173		10. Work Unit No. Proj. No. 034-241-012	11. Contract or Grant No. IAG DOT-FA72WAI-261
12. Sponsoring Agency Name and Address Department of Transportation Federal Aviation Administration Systems Research and Development Service Washington, D.C. 20591		13. Type of Report and Period Covered Project Report	
15. Supplementary Notes The work reported in this document was performed at Lincoln Laboratory, a center for research operated by Massachusetts Institute of Technology under Air Force Contract F19628-70-C-0230.			
16. Abstract <p>This report investigates the requirements imposed on a surveillance system for supporting independent approaches to closely spaced parallel runways. Based on a proposed procedure for monitoring aircraft approach paths and controlling deviations from proper approach paths, the required spacing between runway centerlines is derived as a function of surveillance system characteristics and other parameters. Potential trade-offs between the surveillance system characteristics are then investigated to determine whether the DABS sensor might be utilized for position measurement and/or communication in such a surveillance system. The results indicate that the required runway spacing is more sensitive to delays and data update intervals than to position measurement accuracies, and that, if DABS is to perform the communication function in the system, it should probably be used for position measurement as well.</p>			
17. Key Words Closely spaced parallel runways Surveillance system Discrete Address Beacon System (DABS) Monitoring and control geometry		18. Distribution Statement Availability is unlimited. Document may be released to the National Technical Information Service, Springfield, Virginia 22151, for sale to the public.	
19. Security Classif. (of this report) Unclassified	20. Security Classif. (of this page) Unclassified	21. No. of Pages 56	22. Price 3.00 HC .95 MF



TABLE OF CONTENTS

<u>Section</u>	<u>Page</u>
1. INTRODUCTION.....	1
2. MONITORING AND CONTROL PROCEDURE.....	2
2.1 SPACING CONFIGURATION.....	2
2.2 BLUNDER DETECTION.....	5
2.3 THE RECOVERY ZONE.....	7
2.4 SYSTEM PERFORMANCE MEASURES.....	9
2.5 PHASES OF APPROACH.....	11
3. SENSITIVITY AND TRADE-OFF RESULTS.....	12
3.1 SYSTEM PARAMETERS AND ASSUMPTIONS.....	12
3.1.1 Flight Parameters.....	12
3.1.2 System Probability Parameters.....	14
3.1.3 Surveillance Parameters.....	15
3.2 RUNWAY SPACING SENSITIVITY TO SELECTED SYSTEM PARAMETERS.....	16
3.2.1 Effects of Flight Parameters.....	21
3.2.2 Effects of Surveillance Parameters.....	21
3.3 SURVEILLANCE PARAMETER TRADE-OFFS.....	22
4. CONCLUSIONS AND ADDITIONAL COMMENTS.....	27
4.1 DABS REQUIREMENTS FOR 2500-ft \downarrow SPACING.....	27
4.2 ADDITIONAL COMMENTS.....	28
 <u>Appendix</u>	
A RECOVERY ZONE CALCULATIONS.....	30
A.1 BLUNDER DETECTION.....	30
A.2 THE RECOVERY MANEUVER.....	32
A.3 RECOVERY ZONE WIDTH.....	36

TABLE OF CONTENTS (Continued)

<u>Appendix</u>	<u>Page</u>
B	SOME ESTIMATES OF PERFORMANCE MEASURES..... 39
	B.1 PROBABILITY OF EXCURSION FROM THE NOZ..... 39
	B.2 PROBABILITY OF FALSE ALARM..... 40
	B.3 WAVE-OFF PROBABILITY..... 40
C	RELATIONS BETWEEN TRACKER ERRORS AND SENSOR MEASUREMENT ERRORS..... 45
	LIST OF SYMBOLS..... 50
	REFERENCES..... 52

PARALLEL APPROACH SURVEILLANCE

1. INTRODUCTION

The use of closely-spaced parallel runways for independent IFR operations can significantly increase airport capacity while utilizing the least possible amount of real estate. In the 1969 report [1], the Air Traffic Control Advisory Committee (ATCAC) recommended a centerline spacing of 2500 ft for independent parallel runways used in conjunction with a microwave instrument landing system (MILS). Based on this recommendation it is evident that a highly accurate and reliable monitoring and control system will be required to support safe operations on such closely-spaced approach zones.

In support of the approach control system, measurements of the state of the aircraft must be made available on the ground. Proposed candidates for the position measurement function are:

- (1) Downlinked MILS data.
- (2) DABS sensor data.
- (3) An independent and highly accurate surveillance system
which is specifically designed for approach monitoring.

The downlinking of MILS data can be performed by a separate VHF data link or, more likely, the DABS data link.

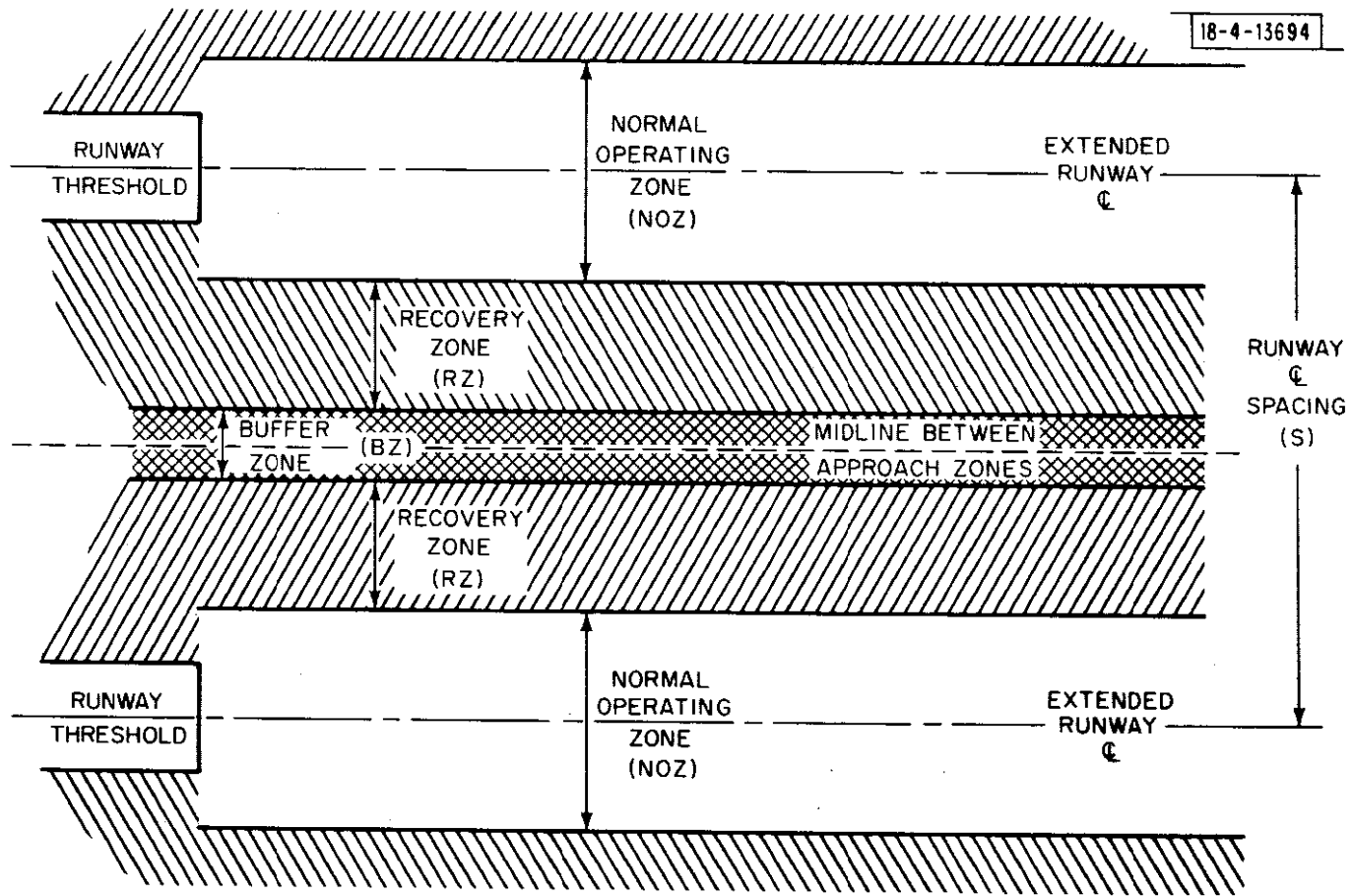
The object of this study is to provide a parametric evaluation of the general surveillance requirements from which the most cost-effective system configuration can be chosen. The surveillance and communication parameters of interest are sensor accuracy, update rate, and data-link delay. We shall place particular emphasis on the question of whether or not the DABS sensor can be expected to meet the stringent requirements necessary to perform this function.

2. MONITORING AND CONTROL PROCEDURE

The model employed for relating the surveillance requirements to spacing of parallel runways is based on the precision of ground tracking and the ability to predict the aircraft's future position through straightline and curved flight paths. The use of position and velocity estimates from the tracker and/or the use of air-derived information make it possible to give earlier valid warnings and/or fewer false warnings than if only position measurements are available. The parallel runway and approach zone configuration is illustrated in Figure 1, and the geometry of the monitoring and control procedure is detailed in Figure 2.

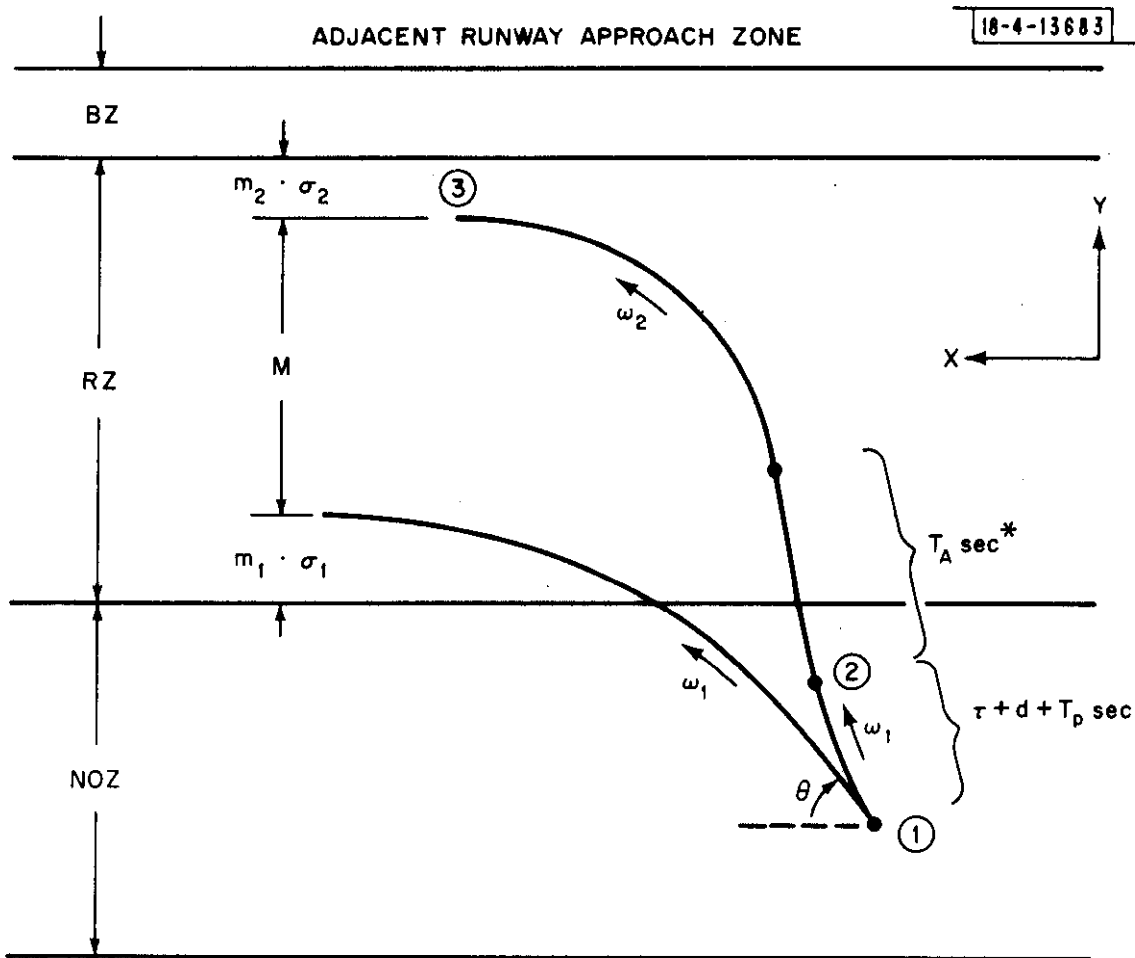
2.1 SPACING CONFIGURATION

Figure 1 shows the three basic zones that contribute to the runway centerline spacing. A Normal Operating Zone (NOZ) is defined; its width must be sufficient to allow normal flight errors expected on final approach. These flying errors depend on the precision of the particular ILS (or MILS) system, pilot and aircraft capabilities, wind effects, wake turbulence, etc. We do not make any



3

Fig. 1. Parallel runway approach zone configuration.



- | | |
|--|---|
| ω_1 = NORMAL TURN RATE | M = MANEUVER DISTANCE |
| ω_2 = RECOVERY TURN RATE | m_1 = FALSE-ALARM PROBABILITY PARAMETER |
| θ = HEADING ANGLE RELATIVE TO ϕ | m_2 = WAVE-OFF PROBABILITY PARAMETER |
| T_p = PILOT REACTION TIME | $\sigma_1 \sigma_2$ = PROJECTED SURVEILLANCE ERRORS |
| τ = SURVEILLANCE SYSTEM UPDATE INTERVAL | NOZ = NORMAL OPERATING ZONE |
| d = DATA LINK DELAY | |
| BZ = BUFFER ZONE | |
| RZ = RECOVERY ZONE | |

* T_A = SECONDS REQUIRED TO ROLL INTO RECOVERY TURN

Fig. 2. Monitoring and control geometry.

detailed analysis of the required NOZ width but, rather, rely on past studies. A "no trespass" Buffer Zone (BZ) separating the two parallel approach zones is also defined; its width must assure minimum "safe" separation in case both aircraft are in coincidental blunder maneuvers.

Between the NOZ and the BZ is a Recovery Zone (RZ) of width dependent on surveillance errors and the distance needed to recover from the worst case blunder which we would like to be correctable with a high degree of certainty. It is important to note that the "worst case blunder" described in the model is not the worst possible potential condition that may occur; it is the worst condition that can be corrected without interfering with aircraft approaching the adjacent runway. The distance required for recovery is dependent upon the maximum turn rate encountered during normal operation, ω_1 , the specified recovery turn rate, ω_2 , the aircraft final approach speed, V , the aircraft roll rate, c_γ , the heading angle, θ , with respect to the runway centerline, the pilot reaction time T_p , the surveillance update interval, τ , and data-link delay, d . In addition, the recovery zone must include sufficient space to absorb surveillance errors which are described below.

2.2 BLUNDER DETECTION

An ideal parallel runway monitoring system would never give a recovery command to an aircraft unless it were indeed going to leave the NOZ and would give the command in a very timely manner so that excursions out of the NOZ would be small. In the design of a practical system, a threshold must be set and a command to turn toward the extended runway centerline must be given if this threshold is exceeded. If the threshold is very low, there will be an

excessively large number of unnecessary commands and perhaps missed approaches. If the threshold is very high, no unnecessary commands will occur but aircraft may frequently embark on a course that will lead to a deep excursion into the RZ before it can recover in response to the command. This either would require a wide RZ and, in consequence, a wide spacing between runways or would require an excessively large number of waveoffs to aircraft on the adjacent runway.

Unlike previous work [2] where this threshold is expressed only in terms of estimates of the present aircraft position, our approach is to make a decision to send a command, based upon whether or not the maximum cross-track excursion of a specific projected aircraft flight path exceeds a threshold. This approach permits the use of cross-track velocity or, equivalently, heading information available from the tracker.

The proposed monitoring system operates as follows (see Figure 2). At each surveillance update point, the position/velocity measurements are used to make a projection of the aircraft flight path. In this projection, it is assumed that the aircraft is executing a normal turn maneuver (turn rate ω_1 , Figure 2) back toward a heading parallel to the extended runway centerline. This projection is used to determine with a specified degree of certainty, that an excursion from the NOZ is unavoidable, even if the pilot is making the proper standard maneuver. The degree of certainty, or, alternately the probability of declaring an impending excursion where there is none, is determined by the distance $m_1 \cdot \sigma_1$, where σ_1 is the standard deviation of error in cross-track position at that point where the projected flight path is parallel to the runway centerline, and m_1 is the specified probability constant. If the projected flight path remains within the $m_1 \cdot \sigma_1$ threshold, no ATC intervention

is required; if it exceeds $m_1 \cdot \sigma_1$, a recovery command is issued. Thus, an unnecessary command is issued, assuming that the normal turn rate ω_1 is not exceeded, only if the error in prediction of the maximum cross-track position exceeds $m_1 \cdot \sigma_1$. This will be a fairly rare event; how rare depends on the value of m_1 chosen.

2.3 THE RECOVERY ZONE

In order to determine the width of the RZ required to ensure that an aircraft will not (with high probability) penetrate the BZ, or adjacent approach zone, it is necessary to analyze the situation described by the postulated worst-case correctable maneuver. Two cases are investigated. The first situation assumes that if, in fact, the aircraft is not in the standard maneuver necessary to stay within the $m_1 \cdot \sigma_1$ control limit at a particular update point (point ① of Figure 2), it will at worst be in a standard rate turn in the opposite direction during the update interval τ . At the next measurement time, the system observes the impending excursion and issues a recovery command. The aircraft continues turning throughout the period of the data-link delay, which is a time of d seconds, that is required for the system to generate and deliver the recovery command to the pilot. An additional delay, T_p , which is the pilot response time, elapses before the pilot can initiate a recovery maneuver (at point ②) in response to the command. The recovery maneuver consists of rolling out of the normal turn toward the adjacent approach zone and into a recovery turn at rate ω_2 , which is greater than the normal turn rate. To determine the required width of the RZ, the flight path is projected through this maneuver until parallel to the runway centerline (at point

③) as shown in Figure 2. The additional lateral distance necessary to execute this maneuver is M . Since this projected flight path is also subject to the errors of the surveillance, we know the maximum cross-track displacement of this maneuver only to an accuracy defined by σ_2 , which is the standard deviation of error in position at that point where the projected flight path is parallel to the centerline. To insure a specified probability of not penetrating the BZ, or adjacent approach zone, we extend the RZ an additional distance of $m_2 \cdot \sigma_2$.

The second blunder maneuver that we consider is simply straightline flight toward the adjacent approach zone. One way to realize straightline blunders as a worst case is to allow for a "do not turn toward the adjacent runway" command at an earlier time when the surveillance system concludes that the aircraft might be heading toward an excursion from the NOZ. This command would require a different threshold than the "do turn" command which is given when the excursion is imminent. The maneuver zone required to correct such a straightline blunder will be smaller than that necessary to correct a turning blunder.

In Appendix A, equations are derived for the width of the maneuver zone, M , and the projected surveillance errors, σ_1 and σ_2 , as a function of the heading angle, θ , the aircraft velocity, V , the roll rate, c_y , elements of the tracker's error covariance matrix, and the other parameters illustrated in Figure 2 ($\tau, d, T_p, \omega_1, \omega_2$). It is also shown that there is a critical heading, θ^* , for which the required RZ width has a maximum, RZ^* . This result is useful since it relieves us of the necessity of limiting the allowable heading. The required runway centerline spacing, S , is then given by

$$S = \text{NOZ} + 2RZ^* + \text{BZ}$$

$$= \text{NOZ} + 2(m_1 \cdot \sigma_1(\theta^*) + M(\theta^*) + m_2 \cdot \sigma_2(\theta^*)) + \text{BZ} \quad (1)$$

In an ideal case where position and velocity are known precisely at each update point, the centerline spacing is required to be 2940 feet, corresponding to the turn-away blunder and the following parameter values: NOZ = 800 ft, BZ = 500 ft, V = 180 knots, $\tau = 1$ sec, $d = 0$ sec, $T_p = 2$ sec, $c_\gamma = 10^\circ/\text{sec}$, $\omega_1 = 1.5^\circ/\text{sec}$, $\omega_2 = 3^\circ/\text{sec}$, $m_1 = 1.0$, and $m_2 = 0$. The remainder of this report describes the sensitivity analysis for the case of imperfect surveillance with the use of the system model and equations described above.

2.4 SYSTEM PERFORMANCE MEASURES

Several performance measures of interest may provide a basis for system design. These are the probability that an aircraft requires a maneuver command, the false alarm probability, and the probability of an unelected blunder. The probability that an aircraft requires a maneuver command (denoted by P_1) is the probability that at a particular update point, the true position/velocity combination is such that the aircraft cannot stay within the NOZ by turning at rate ω_1 back toward the correct heading. This probability depends on the normal flight deviations from ideal approach, as well as the width of the NOZ. As mentioned earlier, the NOZ width must be such as to keep the probability of excursion small. The reasons are twofold. First, the rate of ATC intervention is significant in determining the communications load placed on the data link. And secondly, the expected rate of maneuver commands will have a direct bearing

on pilot acceptance of the overall parallel runway system. Both of these considerations require that the NOZ be large enough to keep P_1 small.

The false alarm probability (P_2) is defined to be the probability of giving the aircraft an unnecessary command conditional on a command being given; i.e., the ratio of unnecessary commands to total commands. This probability depends upon normal flight deviations, surveillance errors, and the system parameter m_1 that was previously discussed. Clearly, false alarms need to be kept at a specified low level.

The third performance measure, the probability of an undetected blunder (P_3), is the most important of the three. By undetected blunder, we mean failure to detect an excursion from the NOZ until it is too late to avoid penetration of the adjacent approach zone, even with a perfectly executed recovery maneuver. The result of such an occurrence is a potentially dangerous situation and probably interference with operations in the adjacent approach zone (such as wave-offs to properly performing aircraft). We define P_3 as the probability of the proper recovery flight path penetrating the adjacent approach zone, conditional on a command being given; i.e., the ratio of wave-offs caused by surveillance errors to the total number of commands. Clearly, this probability must be kept small.

The three performance measures described above can all be expressed mathematically in terms of both the probability distributions of aircraft flight deviations from assigned or ideal approach paths and the surveillance errors. Since the flying error distribution for an aircraft approach on a MILS system is totally unknown at this time, it does not seem reasonable to develop actual numerical values for performance measures with a guess as to the starting

information. Even when a MILS system is in operation, it would probably be more realistic to estimate the performance of the parallel approach monitoring system with actual flight tests. However, for purposes of this study we can get a rough idea of what the expected performance of the proposed system will be. This is discussed in more detail in Appendix B.

2.5 PHASES OF APPROACH

It was noted at the outset of this project that there are two distinct phases to final approach. The first phase is the turn-on phase during which the aircraft first captures the ILS and then turns to the proper approach heading. The second phase of approach is the flight on the ILS to touchdown. We have developed our model to handle either phase (by excluding heading restrictions), but the probable overshoots at turn-on may require an extra margin of safety at that point.

Several procedures can be used to overcome this problem. Altitude separation at turn-on can be provided by means of two different glide slopes (e.g., 2.5° and 3°) and staggered runway thresholds for two simultaneously approaching aircraft. An alternate (or possibly complementary) method is utilization of some type of "time to turn" information prior to actual localizer intercept [3]. A third possibility is to eliminate or greatly reduce overshoots by implementing curved approach paths made possible with MILS equipment.

With one or several of the above ideas assumed implemented for the turn-on phase, we restrict the remainder of this study to the final approach after localizer capture. The proposed system will allow the aircraft to fly within the established NOZ without ATC intervention, but will still protect against

possible blunders with no limitation on heading angle relative to the centerline. Aircraft on the adjacent approach path will be interfered with (waved-off) only when it is evident that a blundering aircraft cannot recover in time to avoid a potential hazard.

3. SENSITIVITY AND TRADE-OFF RESULTS

In this section, we illustrate the sensitivity of required runway spacing to several parameters that may be controlled in a design of the parallel approach monitoring system. Also, for given required runway centerline spacings, we investigate the surveillance parameter trade-offs which are available.

3.1 SYSTEM PARAMETERS AND ASSUMPTIONS

In determining the sensitivity of required runway spacing to the controllable system parameters, we assume a nominal set of parameter values. Each variable of interest can be assigned to one of three general categories: flight parameters, system probability parameters, and surveillance parameters. The following is a brief discussion of each category and its associated nominal parameter value.

3.1.1 Flight Parameters

These variables are characteristics of aircraft and pilot capabilities and in some cases may possibly be limited by airport approach regulations.

- (1) Approach Speed Limit ($V = 180$ knots) - A regulated maximum final approach speed. This value is meant to be an upper bound; similar studies use 150 knots as a "typical" speed.

- (2) Normal Turn Rate ($\omega_1 = 1.5^\circ/\text{sec}$) - A regulated or suggested turn rate under normal conditions. Again, the nominal value is meant to be an upper bound. 1961 NAFEC flight tests at Chicago [4] show the normal turn rate to be about $0.5^\circ/\text{sec}$ during final approach after turn-on.
- (3) Recovery Turn Rate ($\omega_2 = 3^\circ/\text{sec}$) - An assumed turn rate for the recovery maneuver. Although slower aircraft may achieve a faster turn, the nominal value seems to be the maximum that can be expected for the velocities under consideration and for reasonable bank angles (with respect to passenger comfort).
- (4) A/C roll rate ($c_Y = 10^\circ/\text{sec}$) - An assumed rate for rolling into a recovery turn.
- (5) Pilot Response Time ($T_p = 2 \text{ sec}$) - An assumed reaction time measured from the time the pilot receives a warning to the time he initiates the recovery maneuver. This nominal value is believed to be reasonable for such a tightly controlled and critical phase of flight as instrument approach.
- (6) Wind - Wind effects are assumed important only in determining flying errors and consequently the NOZ width.

The only two flight parameters which we have considered controllable are speed, V , and normal turn rate, ω_1 . Therefore, these are the only ones investigated in the sensitivity analysis. The others are held fixed at their nominal values through the study.

3.1.2 System Probability Parameters

The following parameters are the components which actually comprise the runway centerline spacing. Along with the surveillance parameters, they also determine the performance measures discussed previously.

- (1) Normal Operating Zone (NOZ = 800 ft) - The nominal value is based on results in [2] which indicate that 800 ft is sufficient to realize marginally acceptable small excursion rates for present day flight capabilities. Implementation of an 800 ft NOZ in conjunction with a microwave ILS should reduce excursion rates even lower.
- (2) Buffer Zone (BZ = 500 ft) - The nominal value is based on a number of past studies [2].
- (3) Recovery Zone (RZ) - The width of the recovery zone depends on surveillance system accuracy and three additional criteria:
 - (a) False alarm probability parameter ($m_1 = 1.0$) - The nominal value yields a probability of less than 0.1 that a given alarm is unnecessary. See Appendix B for this determination.
 - (b) "Wave-off" or undetected blunder probability parameter ($m_2 = 0.$) - The nominal value is used in conjunction with a 500 ft Buffer Zone in the initial sensitivity analysis and is investigated in detail in Appendix B.
 - (c) Maneuver Zone (M) - This depends on the previously mentioned flight parameters and on which of the two postulated blunders is assumed.

Since the NOZ and BZ widths are strictly additive to the required centerline spacing and the RZ is essentially a function of other system parameters, no sensitivity analysis is required on these spacing parameters.

3.1.3 Surveillance Parameters

These characteristics of the approach surveillance are the requirements of primary interest in this study.

- (1) Update Interval (τ) - Time between successive updates of surveillance information is a variable design parameter. A nominal value of 1 sec is utilized in the initial sensitivity study.
- (2) Data-link Delay (d) - The time to compute and display a warning to the pilot is also a variable design parameter initially set at a nominal value of 1 sec.
- (3) Sensor Accuracy - The two components of measurement accuracy, range and azimuth, are considered separately. If we assume that the sensor is located approximately at the center of the airport, the range accuracy corresponds roughly to the along-track (x-direction in Figure 1) position measurement accuracy, and the azimuth accuracy corresponds to the cross-track (y-direction) position measurement at a specific distance. We use a range of 10 nmi for conversion between azimuth and cross-track position throughout the analysis. If the maximum range coverage for parallel approach monitoring is R nmi, then the azimuth accuracy indicated in certain curves presented in this report must be multiplied by a factor of 10/R.
 - (a) Sensor range accuracy - We assume a 150 ft (1 sigma) range error. Tracker simulation studies have shown a resultant along-track velocity error ($\sigma_{\dot{x}}$) of 6.75 ft/sec. As this error does not greatly affect our results, we use this value throughout the study.

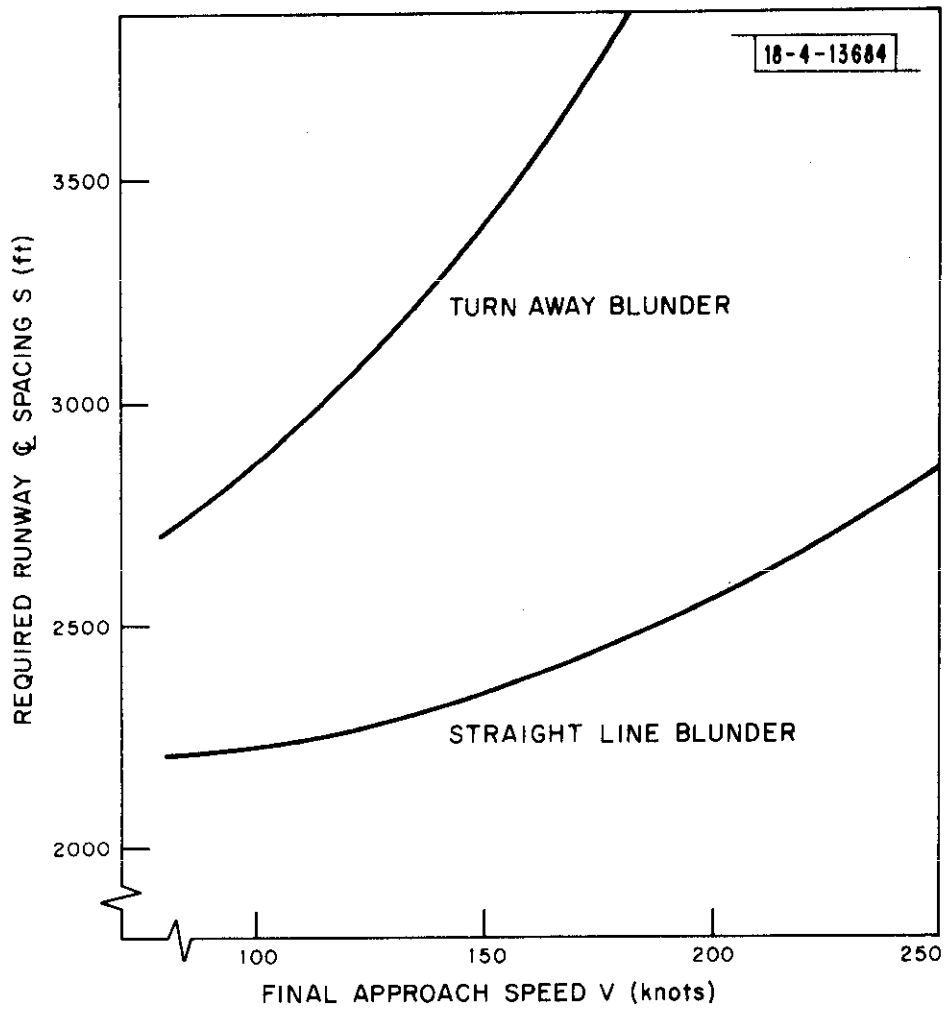
- (b) Sensor azimuth accuracy - This measurement accuracy is a variable design parameter directly affecting both cross-track position accuracy (σ_y) and cross-track velocity accuracy ($\sigma_{\dot{y}}$), both of which significantly affect required runway spacing. The tracker variances $(\sigma_y)^2$ and $(\sigma_{\dot{y}})^2$ are functions of both sensor measurement errors and data update interval. Appendix C discusses the tracker model and derives the relations used in this work. The nominal azimuth accuracy is $\sigma_\theta = 0.2^\circ$ which corresponds to a cross-track position measurement accuracy of $\sigma_m = 213$ ft at 10 nmi.
- (c) Tracker covariance elements - These are given by the product of the component rms error values

$$|\sigma_{y\dot{y}}| = \sigma_y \cdot \sigma_{\dot{y}}$$

corresponding to 100% correlation as a worst case. In actual practice, the values will be somewhat less.

3.2 RUNWAY SPACING SENSITIVITY TO SELECTED SYSTEM PARAMETERS

The sensitivity of required centerline spacing to two flight parameters and all three surveillance parameters is shown in Figures 3 through 6. For each parameter, curves are shown for each of the two proposed blunder maneuvers.



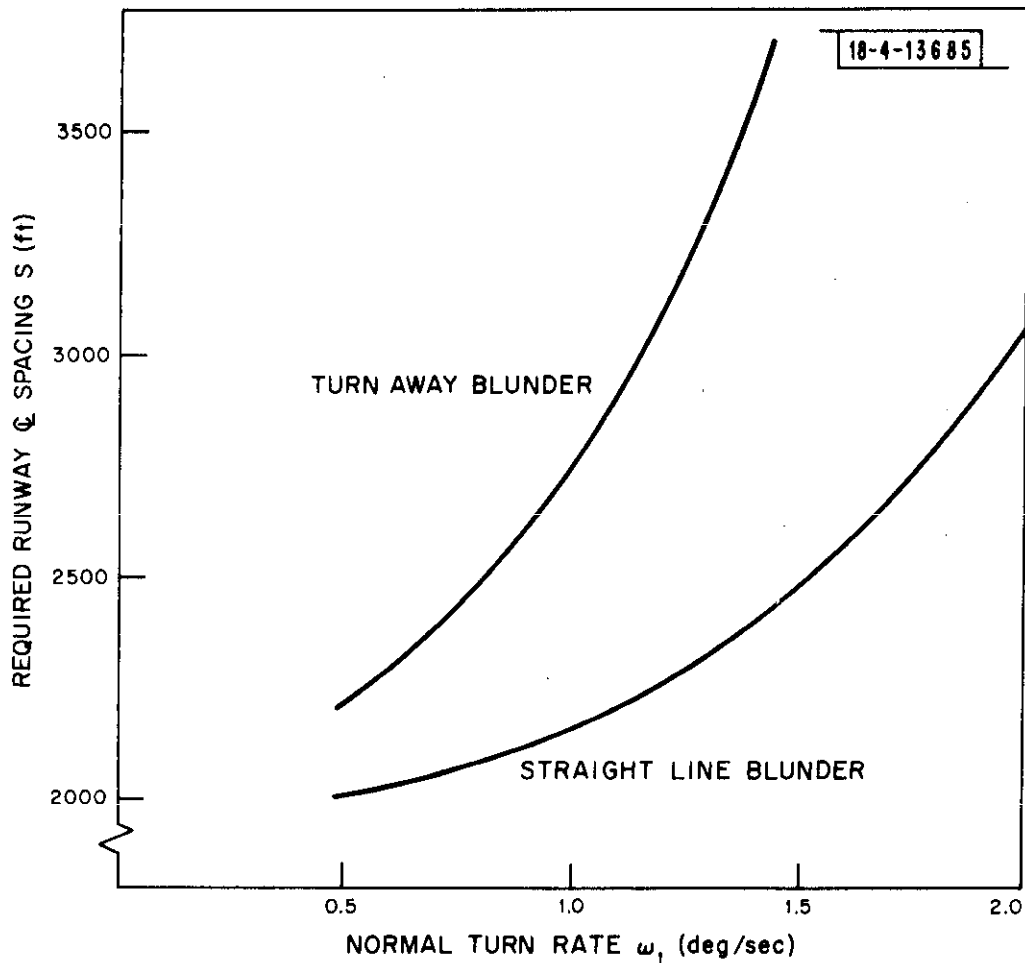
NOMINAL DESIGN PARAMETERS

$\sigma_{\theta} = 0.2^{\circ}$
 $\tau = 1.0 \text{ sec}$
 $d = 1.0 \text{ sec}$

FIXED PARAMETERS

NOZ = 800 ft BZ = 500 ft
 $m_1 = 1.0$ $m_2 = 0.0$
 $\omega_1 = 1.5\%/\text{sec}$ $\omega_2 = 3.0\%/\text{sec}$
 $C_{\gamma} = 10\%/\text{sec}$ $T_p = 2.0 \text{ sec}$

Fig. 3. Required runway spacing vs approach speed.



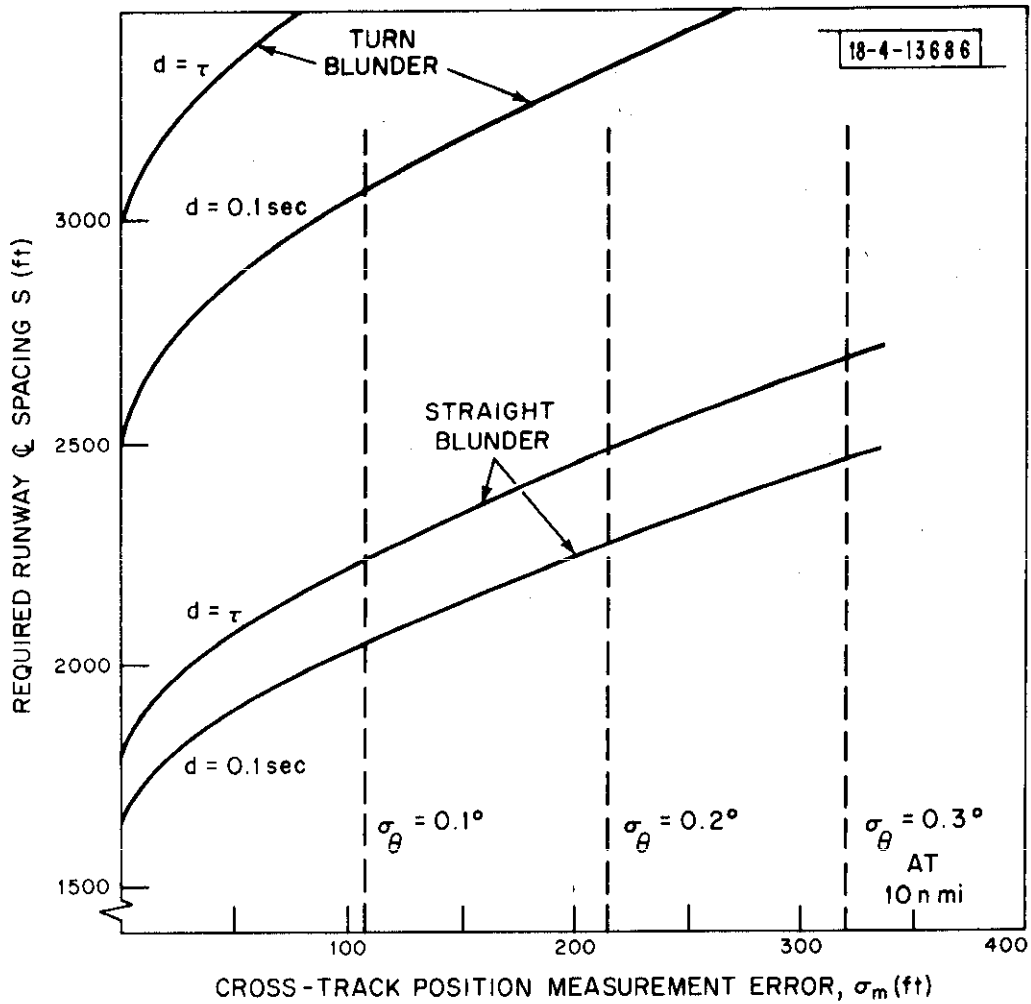
NOMINAL DESIGN PARAMETERS

$\sigma_\theta = 0.2^\circ$
 $\tau = 1.0 \text{ sec}$
 $d = 1.0 \text{ sec}$

FIXED PARAMETERS

NOZ = 800 ft BZ = 500 ft
 $m_1 = 1.0$ $m_2 = 0.0$
 $C_\gamma = 10^\circ/\text{sec}$ $\omega_2 = 3.0^\circ/\text{sec}$
 $T_p = 2.0 \text{ sec}$ $V = 180 \text{ KNOTS}$

Fig. 4. Required runway spacing vs normal turn rate.



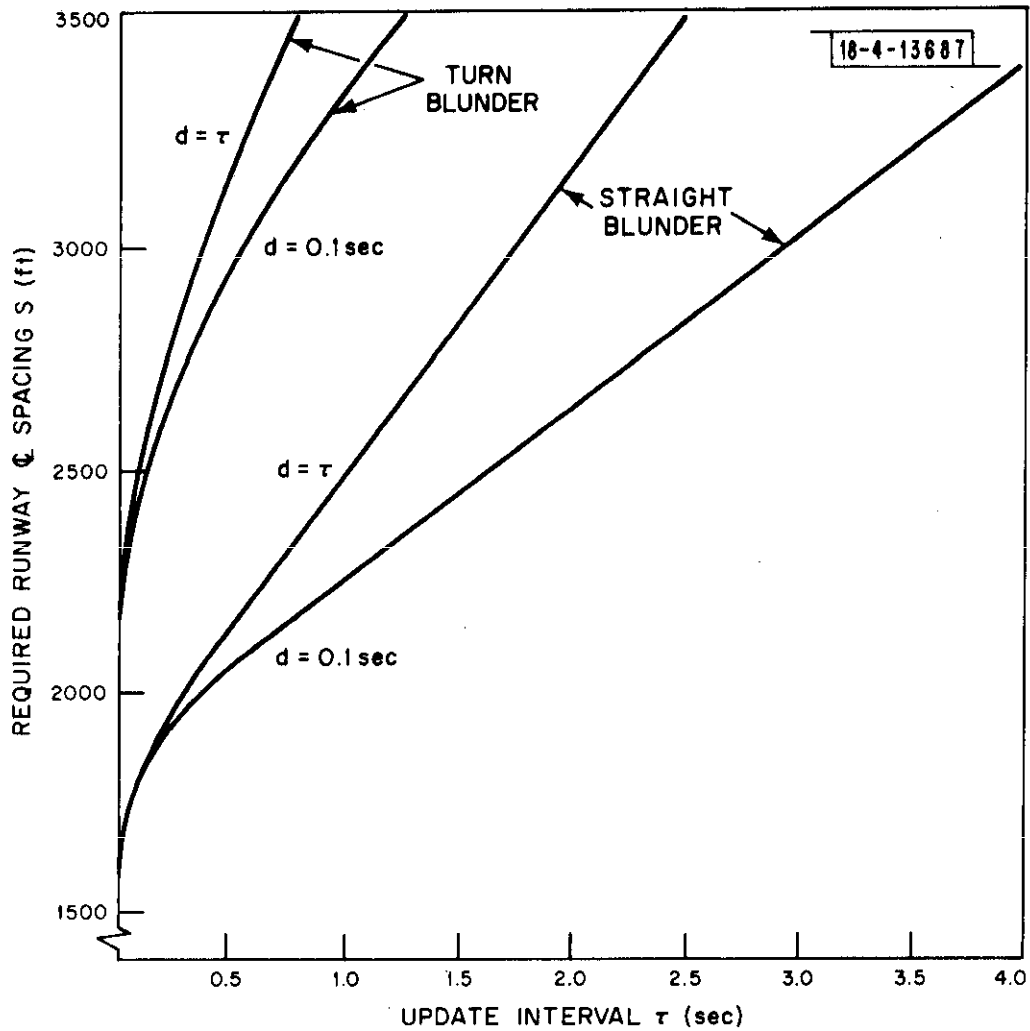
NOMINAL UPDATE TIME

$\tau = 1.0 \text{ sec}$

FIXED PARAMETERS

NOZ = 800 ft BZ = 500 ft
 $m_1 = 1.0$ $m_2 = 0.0$
 $\omega_1 = 1.5 \text{ }^\circ/\text{sec}$ $\omega_2 = 3.0 \text{ }^\circ/\text{sec}$
 $C_\gamma = 10 \text{ }^\circ/\text{sec}$ $V = 180 \text{ KNOTS}$
 $T_p = 2.0 \text{ sec}$

Fig. 5. Required runway spacing vs position measurement.



NOMINAL SENSOR ERROR

$\sigma_{\theta} = 0.2^{\circ}$
 $(\Rightarrow \sigma_m = 213 \text{ ft AT } 10 \text{ nmi})$

FIXED PARAMETERS

NOZ = 800 ft BZ = 500 ft
 $m_1 = 1.0$ $m_2 = 0.0$
 $\omega_1 = 1.5^{\circ}/\text{sec}$ $\omega_2 = 3.0^{\circ}/\text{sec}$
 $C_{\gamma} = 10^{\circ}/\text{sec}$ $V = 180 \text{ KNOTS}$
 $T_p = 2.0 \text{ sec}$

Fig. 6. Required runway spacing vs update interval.

3.1.1 Effects of Flight Parameters

The two flight parameters assumed controllable are maximum A/C approach speed V and the maximum normal turn rate ω_T . Figure 3 shows the relationships between required centerline spacing and approach speed limit for the nominal parameter values. We observe that spacing increases dramatically with speed for the turn blunder, while the increase is much less severe for a straight blunder. Note that 2500 ft spacing is not possible for the case of a turn blunder for even small velocities with the set of nominal parameter values.

In Figure 4, spacing versus ω_T , we find that spacing increases rapidly with increased turn rate for both blunder cases. It is evident that a restriction on ω_T is necessary to realize 2500 ft spacing in this model. For the remainder of the analysis, ω_T is fixed at the value $1.5^\circ/\text{sec}$ and V is fixed at 180 knots.

3.2.2 Effects of Surveillance Parameters

The characteristics of primary importance in the design of the surveillance are sensor azimuth accuracy, sensor update rate, and the data-link delay. Figures 5 and 6 show the sensitivity of required runway spacing to these parameters. The data-link delay is assumed to be equal to either 0.1 sec, which corresponds to a separate VHF data link or DABS data link with variable interrogation rates, or τ sec, which corresponds to a DABS data link with fixed interrogation rates.

Figure 5 demonstrates spacing as a function of cross-track sensor position measurement error σ_m (equivalent to σ_θ at 10 nmi range) for a fixed update interval of 1 sec. We find that for each set of assumptions on data-link delay

and type of blunder, the rate of increase in required spacing with respect to sensor accuracy is roughly the same. The major differences between the four cases are the starting points for negligible sensor error.

The relations between centerline spacing and update interval for fixed sensor accuracy ($\sigma_{\theta} = 0.2^{\circ}$) and for several cases of data-link delay and blunder type are shown in Figure 6. Here, we observe quite different rates of increase in spacing requirements with increased update interval for the four curves. Also, in all cases the rates of increase are very steep over a relatively small interval of update times (3 sec).

The sensitivity curves in Figures 5 and 6 emphasize three major conclusions. First, the turn-away blunder case imposes substantially greater spacing requirements than does the straight line blunder. It appears that the extra logic and computation required to generate "do not turn" commands, to assure straight line blunders at worst, is probably justified by the reduction in spacing requirement. The second conclusion obtained from the curves is that the data update interval is somewhat more important than sensor measurement accuracy, at least for the range of values considered here. Finally, the type of data link is significant for update intervals greater than 0.5 sec.

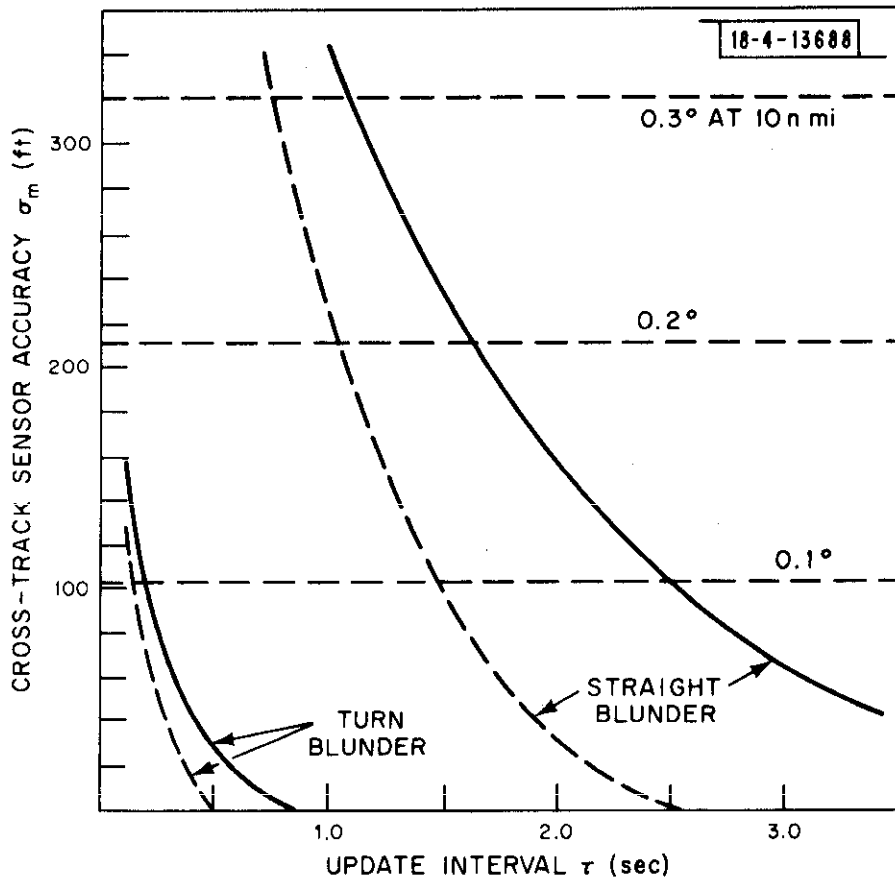
3.3 SURVEILLANCE PARAMETER TRADE-OFFS

The results of the previous sub-section indicate that the update interval may be more important than sensor position measurement accuracy. In this sub-section, we investigate the trade-off available between the two parameters in meeting requirements for supporting certain specified runway centerline spacings. In Figure 7, the curves relating required sensor measurement accuracy to the

data update interval for a 2500-ft runway spacing demonstrate these surveillance system trade-offs for the four combinations of data-link delay and blunder maneuver. As before, we hold the other parameters to their nominal values. It is evident that operating points on either curve for the turn-away blunder will be difficult to realize in practice. Therefore, we shall now restrict our attention to straight line blunders.

The curves in Figure 7 representing the straight line blunder case show very significant trade-offs available between sensor accuracy and update rate. We also observe a relaxation in requirements if the data-link delay is not restricted by the data update rate. Since data-link delay would be dependent on τ for the case of a rotating antenna, it appears that on the basis of this model, a rotating antenna with an update interval greater than two seconds will not support the 2500 ft spacing. If we assume an agile beam antenna, update intervals of one second or less may be realized. Based on Figure 7, this will allow less stringent requirements on sensor accuracy and also possibly better performance, especially with regard to wave-off rates.

For example, the previous results in Figures 3 through 7 were derived on the basis of a 500 ft Buffer Zone but with the "wave-off" probability parameter m_2 set at zero. Coarse performance calculations in Appendix B indicate a probability of wave-off to the adjacent aircraft of roughly 0.08 for a given alarm, corresponding to a sensor accuracy of 0.2° and an update rate of one second. Possibly this is too large a probability of interfering with traffic on the adjacent parallel runway. At least one study [3] suggests a probability of penetration of the adjacent approach zone on the order of 0.001. To realize this value of performance, we must set the parameter m_2 to a higher value but



DATA LINK DELAY

$d = 0.1 \text{ sec}$ ———
 $d = \tau$ - - - -

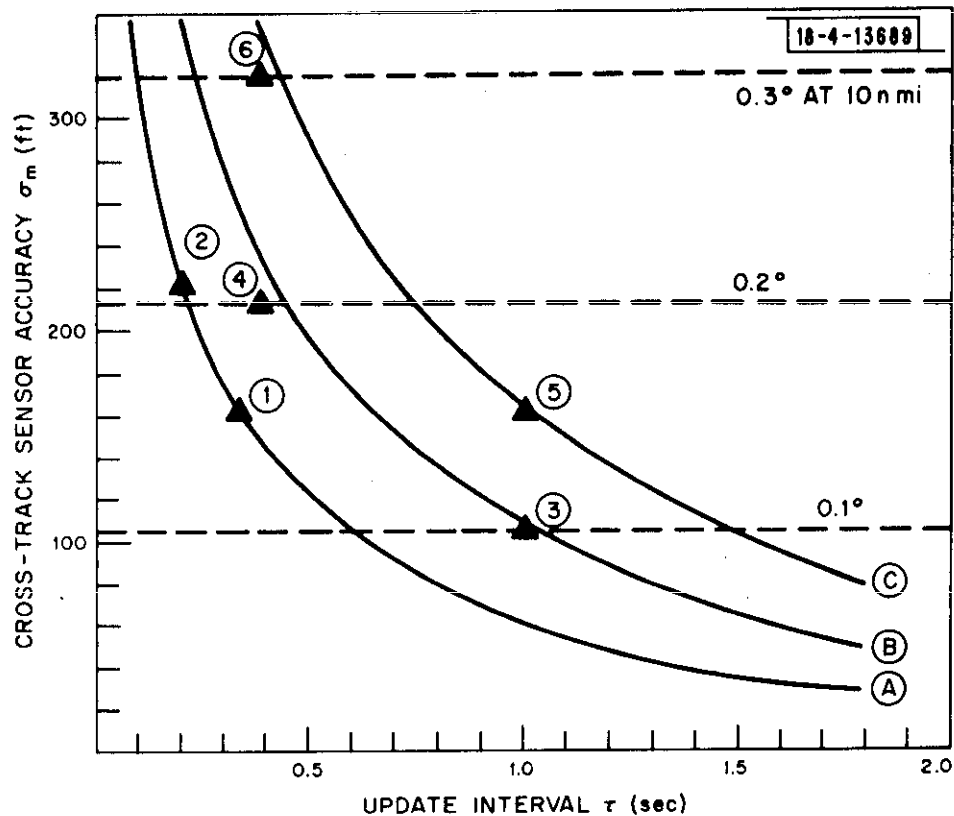
FIXED PARAMETERS

NOZ = 800 ft BZ = 500 ft
 $m_1 = 1.0$ $m_2 = 0.0$
 $\omega_1 = 1.5 \text{ \%sec}$ $\omega_2 = 3.0 \text{ \%sec}$
 $C_\gamma = 10 \text{ \%sec}$ $V = 180 \text{ KNOTS}$
 $T_p = 2.0 \text{ sec}$

Fig. 7. System requirements trade-off for 2500-ft ϕ spacing.

use the midpoint between the approach zones as the threshold boundary. The Buffer Zone may be ignored for the present since the performance requirement is for the single blunder case. Setting m_2 to 3.0 will give a wave-off probability of 0.001 (assuming gaussian errors) for the worst case heading which is generally between 20° and 30° for the reasonable range of parameter values. However, as suggested in Appendix B, the probability of an aircraft having that great a heading deviation is small, so, $m_2 = 3.0$ is probably unnecessarily strict. We choose $m_2 = 2.5$, giving a worst-case wave-off probability of 0.006 and an overall value of about 0.001 (see Appendix B).

Figure 8 shows system trade-off curves of approximately constant performance for the model described above and for several different runway centerline spacings. The blunder is assumed to be straight-line flight and one update interval is allowed for data-link delay. Two possible system operating points are chosen for each curve. For example, for 2500-ft centerline spacing, point (1) requires a sensor azimuth accuracy of 0.15° and three data updates (interrogations if DABS is used) per second. Operation at point (2) relaxes the sensor accuracy to 0.2° but required five updates per second. Similar trade-offs are shown for 3000-ft and 3500-ft centerline spacings. Upon verification of the model assumptions (possibly by actual flight tests), we propose that Figure 8 be utilized for actual design of DABS to provide a monitoring system for supporting closely-spaced parallel approaches.



RUNWAY \mathcal{Q} SPACING

(A) 2500 ft

(B) 3000 ft

(C) 3500 ft

SYSTEM OPERATING POINTS (σ_m, τ)

(1) (0.15°, 1/3 sec); (2) (0.2°, 1/5 sec)

(3) (0.10°, 1 sec); (4) (0.2°, 2/5 sec)

(5) (0.15°, 1 sec); (6) (0.3°, 2/5 sec)

FIXED PARAMETERS

NOZ = 800 ft BZ = 0
 $m_1 = 1.0$ $m_2 = 2.5$
 $\omega_1 = 1.5^\circ/\text{sec}$ $\omega_2 = 3.0^\circ/\text{sec}$
 $C_Y = 10^\circ/\text{sec}$ $V = 180 \text{ KNOTS}$
 $T_p = 2.0 \text{ sec}$ $d = \tau$

STRAIGHT-LINE BLUNDER

Fig. 8. Constant performance system trade-offs for "wave-off" probability ≈ 0.001 .

4. CONCLUSIONS AND ADDITIONAL COMMENTS

The results of the sensitivity and trade-off curves in Section 3 may be applied to any surveillance and communications system proposed for supporting closely-spaced parallel approaches. But since the purpose of this study is to determine what requirement must be met in the DABS design if it is to support these functions, we restrict our conclusions to the several system configurations in which the DABS will have a role. Also, as the stated goal of the ATCAC [1] is 2500-ft spacing of parallel runways, we base the conclusions on this requirement.

4.1 DABS REQUIREMENTS FOR 2500-ft \downarrow SPACING

If DABS is to perform both the surveillance and communications functions, it is evident from Figure 8 that an agile beam antenna will be required. The update interval will probably have to be on the order of 1/5 to 1/3 second (operating points (1) and (2) in Figure 7). The high data refresh rates may cause potential interference and interrogation scheduling problems which need to be investigated.

If DABS is to perform only the communication function in the system, the DABS sensor accuracy has no bearing on the required data rate. However, the type of alternative position measurements employed may place restrictions on the DABS antenna type. If MILS data is to be downlinked via the DABS data link, an update rate on the order of one second is required (see Figure 8 for $\sigma_{\theta} = 0.05^{\circ}$ or [3]). So for this case also, DABS will require an agile beam. For an independent, highly accurate, ground-based approach monitoring system [6] the only function to be performed by DABS is uplinking maneuver commands.

But, here also, we feel that an agile beam antenna would be required if only to provide a reasonably accurate backup surveillance in case of failure of the primary system.

4.2 ADDITIONAL COMMENTS

First, we caution against the use of any results presented here without verification of the fixed assumptions in the model. Two critical areas are the pilot and aircraft capabilities and the tracker model described in Appendix C. Assumptions on the parameters in these portions of the model should be completely verified by actual flight tests.

In the work presented, we have assumed that both position and velocity estimates are derived from sophisticated smoothing of measurements by a sensor located roughly at the center of the airport. Several potential methods of improving the estimates are:

- (1) On-board turn indicator.
- (2) Doppler velocity measurements.
- (3) Multiple sensor coverage.

Any of these could relax the requirements derived in this study. But, even with a relaxation of required update interval to twice the requirements in Figure 7, it is evident that an agile beam antenna will still be required.

An important point which should be subject to further discussion is the desirability of utilizing ground-based surveillance data rather than air-derived MILS data. Faulty MILS equipment on the aircraft or multipath interference on the MILS beam would cause both flying errors and surveillance system errors simultaneously. We feel that the approach monitoring system should be completely independent of the data which the pilot uses for a precision approach.

The conclusions in Section 4.1 indicate that if the DABS sensor is to perform any function in the parallel approach surveillance system, an agile beam antenna will be required. Since very fast update rates are attainable with an agile beam antenna, a surveillance system utilizing DABS sensor measurements at a fast data refresh rate (say, several updates per second) can provide position/velocity estimates as accurately as downlinked MILS data at a one second data rate. Therefore, if DABS is to perform the communication function in the system, it probably should also provide position measurements to ensure the independence discussed above.

APPENDIX A

RECOVERY ZONE CALCULATIONS

The model for blunder detection and recovery is described in the text and illustrated in Figure 2. The Recovery Zone (RZ) is comprised of three parts; the blunder detection error threshold, the maneuver zone, and the recovery error threshold. In this Appendix, we derive the equations for determination of these lateral distances based on the flight path projections for blunder detection and recovery.

A.1 BLUNDER DETECTION

As described previously, at each data update time, we project the aircraft flight path through a normal turn (at rate ω_1) back toward a heading parallel to the extended runway centerline. The maximum lateral position, y_1 , attained in this projection is given by

$$y_1 = y_0 + \frac{V}{\omega_1} (1 - \cos \theta) \quad , \quad (\text{A.1})$$

where

y_0 = initial position

V = speed

θ = heading (relative to centerline).

In terms of the position/velocity components in the x-y coordinate system as estimated by the tracker, the relationship becomes

$$y_1 = y_0 + \frac{(\dot{x}^2 + \dot{y}^2)^{1/2}}{\omega_1} - \frac{\dot{x}}{\omega_1} \quad , \quad (\text{A.2})$$

where

\dot{x} = along-track velocity

\dot{y} = cross-track velocity .

The tracker estimates of y_0 , \dot{y} , and \dot{x} , are all subject to errors due to sensor measurement errors. If the tracker errors are assumed gaussian, we can approximate the error variance with

$$\begin{aligned} \text{Var}(y_1) = \sigma_1^2(\theta) = & \sigma_y^2 + \sigma_{\dot{y}}^2 \frac{\sin^2 \theta}{\omega_1^2} + \sigma_{\dot{x}}^2 \frac{(\cos \theta - 1)^2}{\omega_1^2} \\ & + 2 \sigma_{y\dot{y}} \frac{\sin \theta}{\omega_1} + 2 \sigma_{y\dot{x}} \frac{(\cos \theta - 1)}{\omega_1} \\ & + 2 \sigma_{\dot{y}\dot{x}} \frac{(\sin \theta)(\cos \theta - 1)}{\omega_1^2} \quad . \quad (\text{A.3}) \end{aligned}$$

And if we assume 100% correlations (see sub-section 3.1) with the signs giving the largest total error variance (i.e., worst case), then

$$\sigma_1^2(\theta) = \left(\sigma_y + \sigma_{\dot{y}} \frac{\sin \theta}{\omega_1} + \sigma_{\dot{x}} \frac{(1 - \cos \theta)}{\omega_1} \right)^2 \quad . \quad (\text{A.4})$$

Since y_1 is a non-linear function of the tracker estimates, the distribution of error is not quite gaussian and will have a slight bias. But in a study undertaken to determine whether the distribution might be realistically approximated by a gaussian distribution, it was found that the bias is small and for tail probabilities up to about 3σ , the gaussian approximation is quite good (within 1% or 2%). With the "false alarm" parameter m_1 set to yield the desirable false alarm rate, a blunder is detected if

$$y_1 > y_N + m_1 \cdot \sigma_1(\theta) \quad , \quad (A.5)$$

where

$$y_N = \text{cross-track position of NOZ edge.}$$

A.2 THE RECOVERY MANEUVER

The flight path projection (for a turn-away blunder) through the recovery maneuver is drawn in detail in Figure A.1. The decision (blunder detection) point is at point ①, but to allow for the distance beyond the threshold that the detection projection may fall, we include the part of the trajectory from point ② to point ① through one update interval. Between point ② and point ③ the aircraft continues to turn away through the delay period. The lateral distance travelled before the pilot begins to turn back is

$$\frac{V}{\omega_1} (1 - \cos \theta_1) - \frac{V}{\omega_1} (1 - \cos \theta) \quad .$$

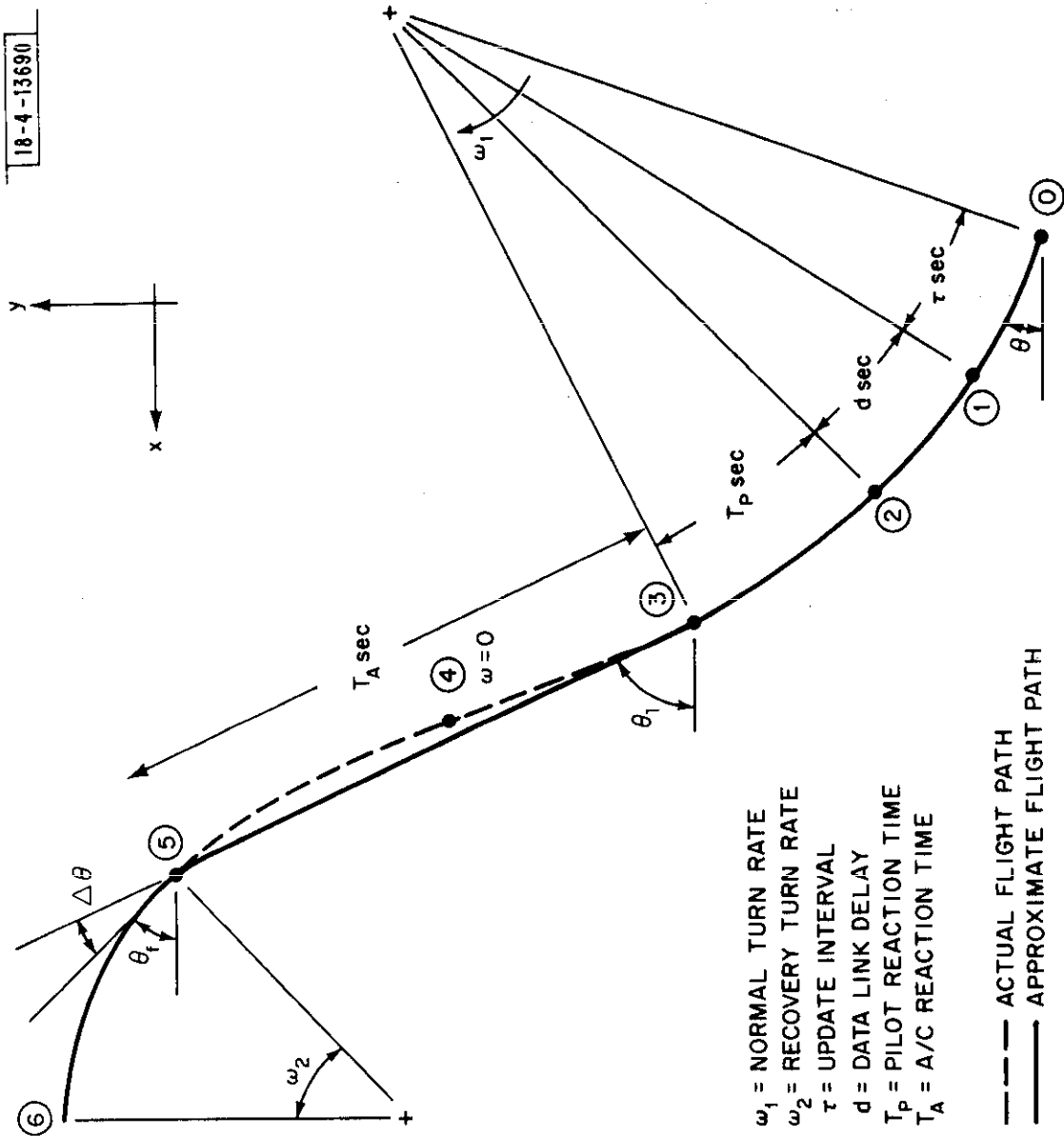


Fig. A.1. Geometry of the recovery maneuver.

At point ③ the aircraft begins to roll (at roll rate c_Y) out of the blunder turn and into the recovery turn. The exact equations of motion between point ③ and point ⑤ have been derived and found excessively complex. But a good approximation to the actual flight path is given by straight line flight at heading θ_1 to point ⑤ and then an abrupt change (decrease) in heading by amount $\Delta\theta$. The time in the straight part of the approximation is T_A , the aircraft response time to roll out of the blunder turn into the recovery turn, and is approximated by

$$T_A \approx \frac{V(\omega_1 + \omega_2)}{c_Y \cdot g} \quad , \quad (A.6)$$

where

c_Y = A/C roll rate

g = gravitational constant .

The heading change $\Delta\theta$ introduced at point ⑤ is approximated by

$$\Delta\theta \approx \frac{V}{2 c_Y \cdot g} (\omega_2^2 - \omega_1^2) \quad . \quad (A.7)$$

Then the lateral distance travelled through the recovery turn, point ⑤ to point ⑥ , is $\frac{V}{\omega_2} (1 - \cos \theta_f)$ where $\theta_f = \theta_1 - \Delta\theta$.

The cross-track position attained at the end of the recovery maneuver, y_2 at point ⑥ , is given by the sum of the three elements of the flight path.

$$y_2 = y_0 + \frac{V}{\omega_1} (\cos \theta - \cos \theta_1) + V \cdot T_A \cdot \sin \theta_1 + \frac{V}{\omega_2} (1 - \cos \theta_f) \quad , \quad (A.8)$$

where

$$\theta_1 = \theta + \omega_1 (T_p = d + \tau) \quad ,$$

$$\theta_f = \theta_1 - \Delta\theta \quad ,$$

$$\Delta\theta = \frac{V}{2 c_\gamma \cdot g} (\omega_2^2 - \omega_1^2) \quad ,$$

$$T_A = \frac{V(\omega_1 + \omega_2)}{c_\gamma \cdot g} \quad .$$

For the case of a straight-line blunder, the flight path from point ① to point ⑤ is a straight line. The final cross-track position is given by

$$y_2 = y_0 + V \cdot (T_A + T_p + d + \tau) \cdot \sin \theta + \frac{V}{\omega_2} (1 - \cos \theta_f) \quad , \quad (A.9)$$

where

$$T_A = \frac{V \omega_2}{c_\gamma \cdot g} \quad ,$$

$$\theta_f = \theta - \Delta\theta = \theta - \frac{V \omega_2^2}{2 c_\gamma \cdot g} \quad .$$

As in the blunder detection projection, the maximum cross-track position in the recovery projection is subject to errors in the position/velocity estimates. Again, assuming gaussian tracker errors, worst case correlations, etc., we can approximate the error variance $\sigma_2^2(\theta)$ of y_2 . Since, in the

text, $\sigma_2(\theta)$ is utilized only for the straight line case, we approximate the variance for that case by

$$\sigma_2^2(\theta) = \left[\sigma_y + \sigma_{\dot{y}} \left(T + \frac{\sin \theta}{\omega_2} \right) + \sigma_{\dot{x}} \frac{(1 - \cos \theta)}{\omega_2} \right]^2, \quad (\text{A.10})$$

where $T = T_A + T_p + d + \tau$, and some small order terms are omitted.

The maneuver zone M in Figure 2 is given by the difference in maximum cross-track positions attained in the two projections. Since the positions, y_1 and y_2 , are functions of heading, M is also a function of heading and for the turn blunder is given by

$$M(\theta) = \frac{V}{\omega_1} (2 \cos \theta - \cos \theta_1 - 1) + V \cdot T_A \cdot \sin \theta_1 + \frac{V}{\omega_2} (1 - \cos \theta_f) . \quad (\text{A.11})$$

For the straight blunder, the maneuver zone becomes

$$M(\theta) = V \cdot (T_A + T_p + d + \tau) \cdot \sin \theta + \frac{V}{\omega_2} (1 - \cos \theta_f) - \frac{V}{\omega_1} (1 - \cos \theta) \quad (\text{A.12})$$

A.3 RECOVERY ZONE WIDTH

For the case of perfect surveillance $\sigma_1(\theta)$ and $\sigma_2(\theta)$ are zero, and the required recovery zone width is given by the maximum maneuver zone. For example, consider the turn away blunder; the maximum $M(\theta)$ can be found by setting the derivative (w.r.t. θ) equal to zero.

$$\frac{d M(\theta)}{d \theta} = \frac{V}{\omega_1} (\sin \theta_1 - 2 \sin \theta) + V \cdot T_A \cdot \cos \theta_1 + \frac{V}{\omega_2} (\sin \theta_f) , \quad (A.13)$$

$$\theta_1 = \theta + \omega_1 \cdot (T_p + d + \tau) = \theta + C_1 ,$$

$$\theta_f = \theta + \omega_1 \cdot (T_p + d + \tau) - \frac{V}{2 c_Y \cdot g} (\omega_2^2 - \omega_1^2) = \theta + C_2 .$$

Therefore,

$$\sin \theta_1 = \sin \theta \cos C_1 + \cos \theta \sin C_1 ,$$

$$\cos \theta_1 = \cos \theta \cos C_1 - \sin \theta \sin C_1 ,$$

$$\sin \theta_f = \sin \theta \cos C_2 + \cos \theta \sin C_2 .$$

Substituting and setting the derivative equal to zero gives a critical angle at which $M(\theta)$ reaches a maximum given by

$$\tan \theta^* = \frac{\frac{\sin C_1}{\omega_1} + T_A \cos C_1 + \frac{\sin C_2}{\omega_2}}{T_A \sin C_1 + \frac{(2 - \cos C_1)}{\omega_1} - \frac{\cos C_2}{\omega_2}} . \quad (A.14)$$

Evaluating θ^* and substituting back into Eq. (A.11) gives the maximum required maneuver zone and thus, recovery zone.

For the realistic case of imperfect surveillance, the recovery zone is made up of the maneuver zone and error thresholds specified by the parameters m_1 and m_2 .

$$RZ = m_1 \cdot \sigma_1(\theta^*) + M(\theta^*) + m_2 \cdot \sigma_2(\theta^*) \quad (A.15)$$

For the range of parameters considered in the sensitivity and trade-off studies of Section 3, the expression in (A.15) reaches a maximum value for θ^* roughly in the range between 20° and 30° . The maximized recovery zone width is used for determining required runway centerline spacing throughout this paper.

APPENDIX B

SOME ESTIMATES OF PERFORMANCE MEASURES

In this Appendix we obtain coarse estimates of the performance measures discussed in Section 2. Exact analytical derivations of these measures is not feasible due to lack of the distribution of the flying errors for an aircraft on final approach and also due to the introduction of the gaussian error assumption for the projection errors as discussed in Appendix A. But rough estimates of the performance probabilities can be obtained by making several simplifying assumptions on flight paths.

B.1 PROBABILITY OF EXCURSION FROM THE NOZ

In order to determine intervention rates for the parallel approach monitoring system, we would need a complete joint distribution of position/velocity states to determine how often the blunder detection threshold would be crossed for a fixed NOZ width. With no data on the distribution of such navigation capabilities we can instead use the estimate given in [2]: for an NOZ of 800 ft, the probability that an aircraft leaves the NOZ is roughly 0.087. This value is based on some actual observed flying errors, and as it is expected that aircraft may perform somewhat better on a MILS system, we take this value to be an estimate of the upper bound. Therefore,

$$P_1 < 0.087 \tag{B.1}$$

B.2 PROBABILITY OF FALSE ALARM

The probability that a given alarm is unnecessary depends on the blunder detection threshold parameter m_1 and also on the flying error distribution. For the purposes of this coarse calculation, we make one simplifying assumption, which is questionable but hopefully approximate to the real situation. Assume that at the time a warning is given, the pilot is equally likely to be either "right" or "wrong." Then, for the straight line blunder, the aircraft is either (1) turning at $1.5^\circ/\text{sec}$ back toward the centerline, or (2) flying straight at the observed heading; each state having a probability of $1/2$. Since the variable threshold for warning is set at $\sigma_1(\theta)$, one standard deviation of the projected error for observed heading θ , the probability that the alarm is unnecessary for state (1) is obtained from tables as 0.159. For state (2), the warning is false with zero probability, as that flight path will carry the aircraft out of the NOZ with certainty. Thus, the rough approximation to the probability that a given alarm is false is

$$P_2 = \frac{1}{2} (0.159) = 0.080 \quad . \quad (B.2)$$

The nominal value $m_1 = 1.0$ seems reasonable.

B.3 WAVE-OFF PROBABILITY

As discussed in Section 2, a wave-off is assumed to be given to the aircraft on the adjacent track if the blundering aircraft cannot, with a correctly executed recovery maneuver, remain on the proper side of the midline between the approach zones. In this case, the cause of penetration of the adjacent

approach zone is the surveillance system error and the resultant maximum cross-track displacement through the recovery maneuver. The probability of such an event depends on the space available for executing the recovery maneuver and the projected error variance of the cross-track displacement of the recovery maneuver, both of which depend on heading at the time of the warning.

Figure B.1 shows the spacing and projections at the time of the warning for an observed heading θ . The recovery projection misses the adjacent approach zone by the distance $x(\theta)$ which acts as the recovery error threshold. To determine the probability of crossing the midline, we measure the miss distance in terms of number of standard deviations of error by which the recovery maneuver misses the midline, $x(\theta)/\sigma_2(\theta)$. As mentioned in Appendix A, there is a critical heading angle for which $x(\theta)/\sigma_2(\theta)$ is at a minimum for any fixed spacing.

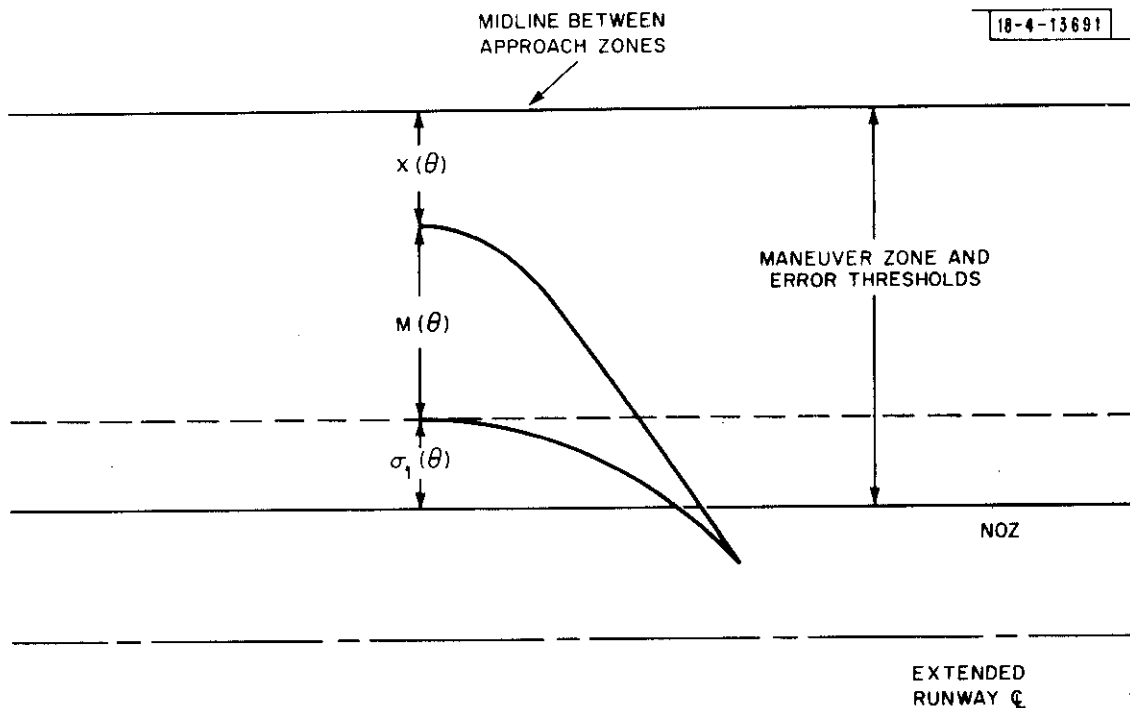


Fig. B.1. Recovery projection miss distance.

For the case in which the parameter m_2 is set at zero, the worst-case-heading miss distance is fixed at one half the width of the buffer zone. Thus, the buffer zone serves two functions; it acts as the worst case heading error threshold as well as a non-penetration zone for the case of simultaneously blundering aircraft on each track. We wish to evaluate the probability of crossing the midline for the single blunder case. For the example calculation, we use the spacing required for the straight line blunder with all parameters set at their normal values (see Figure 5 with $\sigma_\theta = 0.2^\circ$, for example).

The required runway centerline spacing is found to be 2480 ft, of which 840 ft is utilized for the error threshold/maneuver zone for each track. Using the equations of Appendix A, we determine the mean miss distance $x(\theta)$ subject to heading angle by

$$x(\theta) = [840 - M(\theta) - \sigma_1(\theta)] \quad (B.3)$$

To determine the probability that the recovery path actually penetrates the adjacent approach zone, convert $x(\theta)$ into units of standard deviations of error of the recovery projection and obtain the probability from tables of the gaussian distribution. For example, for an observed heading $\theta = 5^\circ$, the distance calculated are $\sigma_1(\theta = 5) = 156$ ft, $M(\theta = 5) = 137$ ft, and $\sigma_2(\theta = 5) = 252$ ft. Therefore,

$$\frac{x(\theta = 5)}{\sigma_2(\theta = 5)} = 2.17 \text{ standard deviations} \quad (B.4)$$

Then the probability of crossing the midline is

$$\Pr\{Z > 2.17\} = 0.0150 \quad , \quad (B.5)$$

where Z is the standard normal random variable. As before, assume that the probability of the aircraft actually being in the straight line blunder when the warning is given is $1/2$. So the probability of wave-off for observed heading of 5° is

$$P_3(\theta = 5^\circ) = \frac{1}{2}(0.0150) = 0.0075 \quad . \quad (B.6)$$

Since the above calculation depended on what heading θ was observed at the time of ATC intervention, we need to assume some probability distribution for observed heading at the warning point. For simplicity, assume a uniform discrete density function

$$\Pr(\theta) = \frac{1}{6} \quad \theta = 5^\circ, 10^\circ, 15^\circ, 20^\circ, 25^\circ, 30^\circ \quad . \quad (B.7)$$

We expect that this is a conservative assumption with the realistic case being a decreasing function of θ with very little probability for $\theta > 30^\circ$.

With the above assumptions, the coarse calculations for wave-off are summarized in Table B-1.

Table B-1. Wave-off Probability Calculations.

θ	$\frac{x(\theta)}{\sigma_2(\theta)}$	$\Pr\{Z \geq \frac{x(\theta)}{\sigma_2(\theta)}\}$	$\times \frac{1}{2} \times \frac{1}{6} = \Pr\{\text{wave-off}, \theta\}$
5°	2.17	0.0150	0.0013
10°	1.43	0.0764	0.0064
15°	0.98	0.1635	0.0136
20°	0.74	0.2296	0.0191
25°	0.67	0.2514	0.0209
30°	0.72	0.2358	<u>0.0196</u>
			$\Sigma = 0.0809$

Therefore, the very approximate probability of a wave-off is $P_3 = 0.081$, for a 500 ft Buffer Zone with $m_2 = 0$.

If, as discussed in Section 4, it is desirable to realize a value of P_3 on the order of 0.001, the error threshold for the recovery projection, and consequently runway centerline spacing, must be increased. To determine the required spacing for this wave-off probability, we set the worst-case-heading error threshold at $x(\theta^*)/\sigma_2(\theta^*) = 2.5$. The required spacing was determined to be 3960 ft for the nominal parameter values, with 1580 ft utilized for absorbing the error in recovery projection. Repeating the above calculations for this spacing, we obtain a wave-off probability of 0.001. Therefore, the final trade-off curves in Figure 7 are developed using the value $m_2 = 2.5$ to realize this small probability of interference with the adjacent approach zone due to surveillance errors.

APPENDIX C

RELATIONS BETWEEN TRACKER ERRORS AND SENSOR MEASUREMENT ERRORS

The object of this Appendix is to derive approximate analytical relationships for the tracker error variances (for cross-track position and velocity) in terms of the sensor's cross-track position measurement error σ_m and the update interval τ . Singer's parametric curves (Figures 3 and 4 of [5]) for a Kalman filter tracker are utilized in conjunction with a tracker simulation. The latter was required to determine the level of random acceleration noise and the value of the correlation coefficient that was needed for the Kalman filter tracker to follow worst-case aircraft maneuvers during an approach to a runway. For various flight paths with maximum turn rates of $1.5^\circ/\text{sec}$ and an update interval of 1 sec, the following Kalman filter parameters resulted in good tracking performances:

$$\alpha \text{ (correlation coefficient)} = 0.1$$

$$\sigma_{\text{man}} \text{ (maneuver noise variance)} = 2.2$$

$$\frac{\sigma_y}{\sigma_m} \text{ (normalized position error)} = 0.6$$

$$\frac{\sigma_{\dot{y}}}{\sigma_m} \text{ (normalized velocity error)} = 0.22$$

With this calibration point and with α and σ_{man} held fixed, Figures 3 and 4 of [5] can now be used to get relations for σ_y and $\sigma_{\dot{y}}$. Since all the logarithmic curves for σ_y vs. the update interval τ are approximately parallel to one another and linear over the region of interest

$$\left(\tau < 4 \text{ sec, } \sigma_m > 50 \text{ ft or } \frac{\sigma_{man}^2}{\sigma_m^2} < 10^{-3} \right),$$

as shown in Figure C.1, the following equation can be written:

$$\frac{\sigma_y^2}{\sigma_m^2} = \left[\frac{\sigma_y^2}{\sigma_m^2} \Big|_{\tau = 1} \right] \tau^{3/4} \quad (C.1)$$

The term $\frac{\sigma_y^2}{\sigma_m^2} \Big|_{\tau = 1}$ is a function of the parameter $\frac{\sigma_{man}^2}{\sigma_m^2}$ in a way shown by

Figure C.2. Since the logarithmic curve is approximately linear, it can be represented by the equation:

$$\frac{\sigma_y^2}{\sigma_m^2} \Big|_{\tau = 1} = \left(\frac{\sigma_{man}^2}{\sigma_m^2} \right)^{0.18} \quad (C.2)$$

By combining the above equations and using the experimentally derived value of σ_{man} , the following equation for the cross-track position error results:

$$\sigma_y = 1.014 \tau^{0.375} \sigma_m^{0.82} \quad (C.3)$$

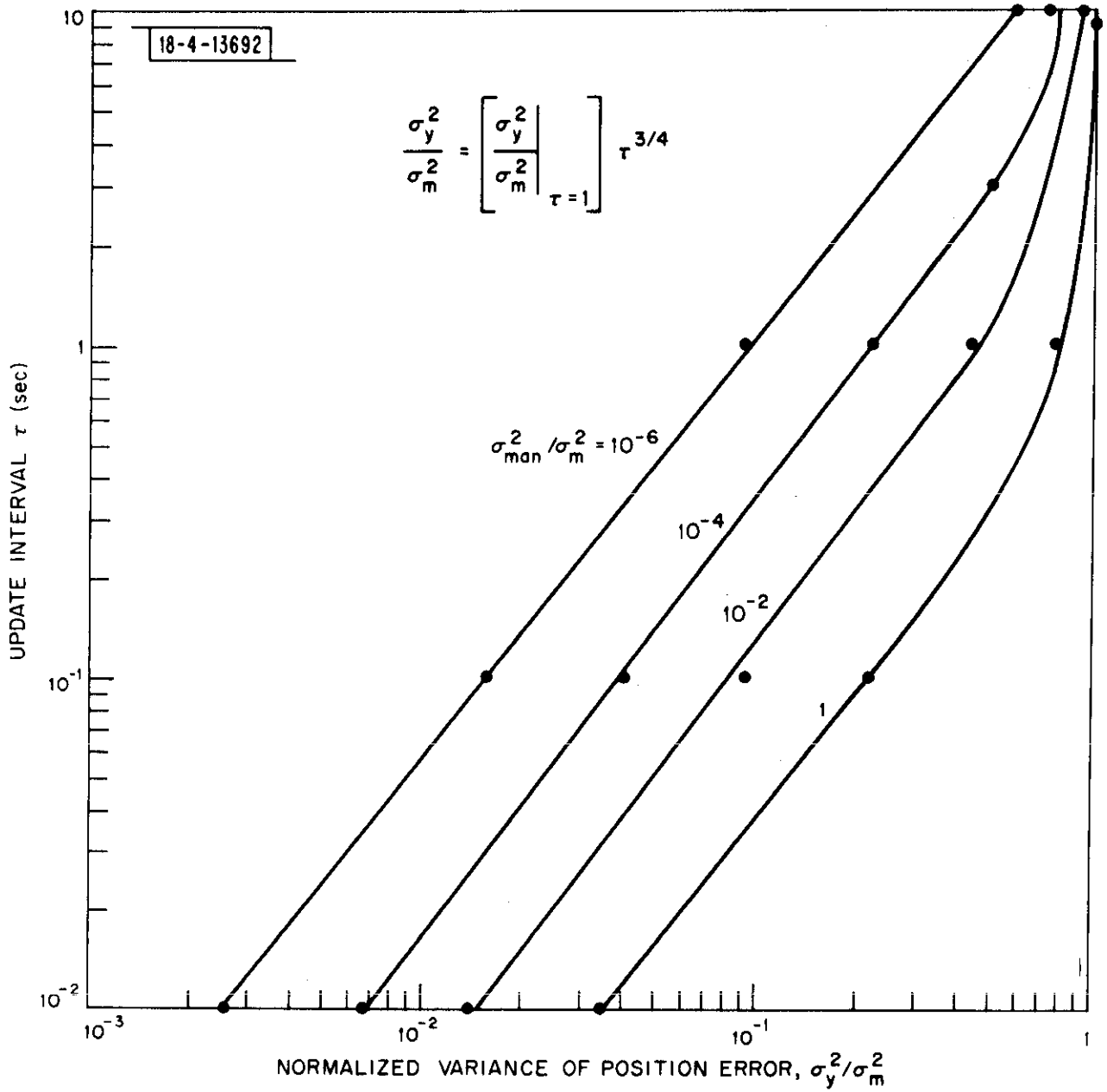


Fig. C.I. Normalized variance of position error vs update interval.

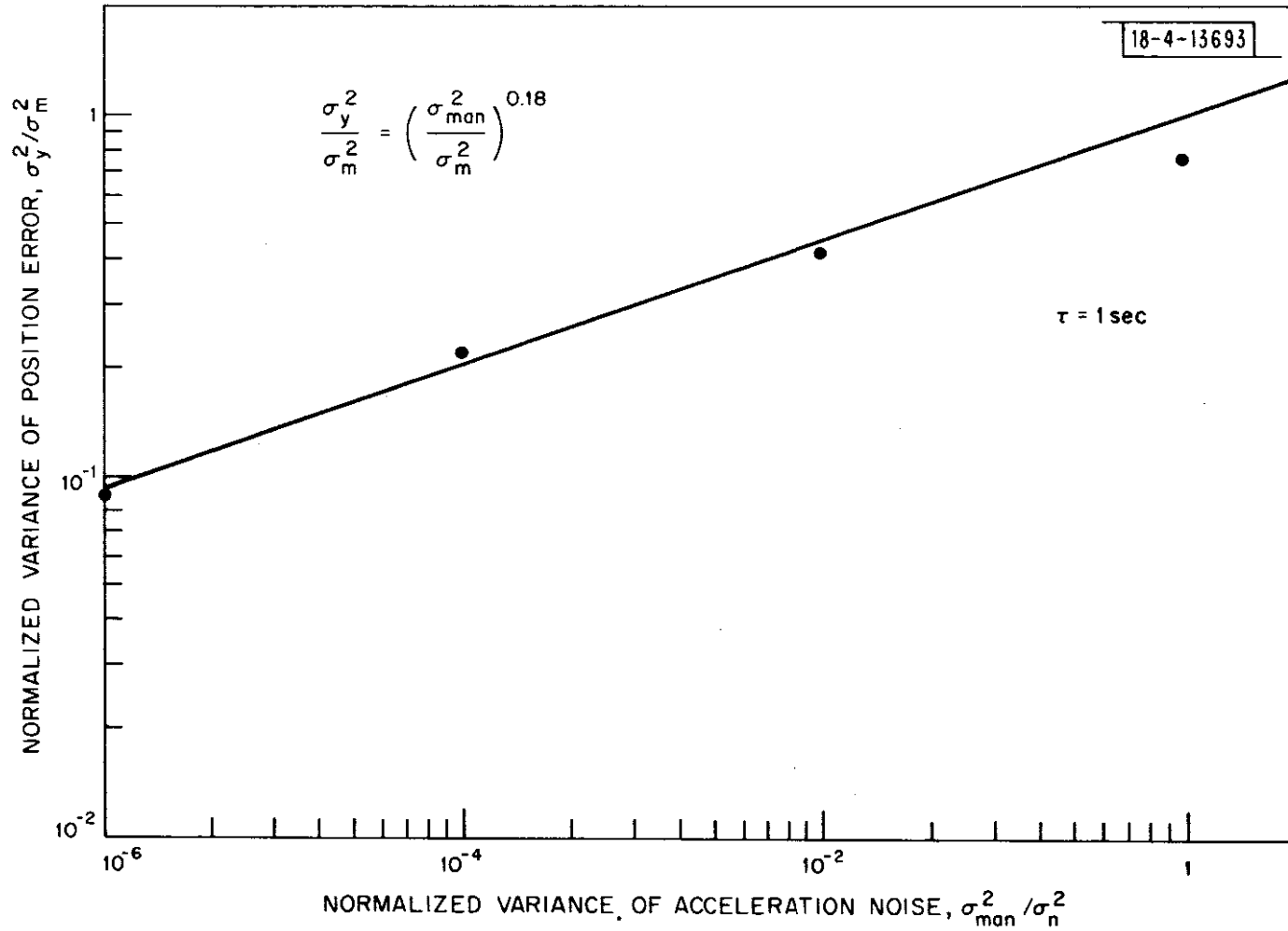


Fig. C.2. Normalized variance of position error vs normalized variance of acceleration noise.

Since the logarithmic curves for σ_y vs. τ are also linear and parallel to one another, they can be treated in the same way as was done above. The resulting equation for the velocity error is:

$$\sigma_y = 1.32 \tau^{0.22} \sigma_m^{0.5} \quad (C.4)$$

LIST OF SYMBOLS

V	Aircraft velocity
ω_1	Normal turn rate
ω_2	Recovery turn rate
c_Y	Aircraft roll rate
T_p	Pilot reaction time
T_A	Aircraft response time
NOZ	Normal operating zone
BZ	Buffer zone
RZ	Recovery zone
M	Maneuver distance
m_1	False-alarm probability parameter
m_2	Wave-off probability parameter
τ	Data update interval
d	Data link delay
σ_{\ominus}	Sensor azimuth measurement error
σ_m	Sensor position measurement error (corresponding to σ_{\ominus} at fixed range)

LIST OF SYMBOLS (Continued)

$\sigma_y, \sigma_{\dot{y}}, \sigma_x$	Tracker estimation errors in position and velocity coordinates
σ_1, σ_2	Estimation errors in maximum cross-track positions attained in the flight path projections
θ	Heading angle relative to \hat{c}
P_1	Probability of ATC intervention
P_2	False alarm probability
P_3	Undetected blunder (wave-off) probability

REFERENCES

- [1] Report of the DOT Air Traffic Control Advisory Committee (ATCAC), December, 1969.
- [2] Kulke, Minkoff, Haroules, "Accurate Surveillance in the Terminal Area," Final Report No. DOT-TSC-FAA-71-26, September, 1971.
- [3] MITRE Corporation, "Recommendations Concerning Reduction of Parallel Runway Spacing under IFR Conditions," MTR-6178, May, 1972.
- [4] Fantoni, J.A., Rudich, R.D., "Evaluation of Parallel Runway Spacing," FAA, NAFEC (ARDS), July 1961.
- [5] Singer, Robert A., "Estimating Optimal Tracking Filter Performance for Manned Maneuvering Targets," IEEE Trans. on Aerospace and Electronic Systems, Vol. AES-6, No. 4, pp. 473-483, July 1970.
- [6] "Performance Monitor of Final Approach, Touchdown and Rollout," Proposal to the FAA from Westinghouse Electric Corporation, Aerospace and Electronic Systems, June, 1971.